

# Electrostatically tunable magnetolectric inductors with large inductance tunability

J. Lou, D. Reed, M. Liu, and N. X. Sun<sup>a)</sup>

Department of Electrical and Computer Engineering, Northeastern University, Boston, Massachusetts 02115, USA

(Received 9 December 2008; accepted 2 March 2009; published online 19 March 2009)

A class of electrostatically tunable inductors with multiferroic composite cores consisting of Metglas/lead zirconate titanate/Metglas was demonstrated. These magnetolectric inductors exhibit a large tunable inductance range  $\Delta L/L_{\min}$  of up to 450%, together with improved quality factors. Such tunability of inductance and quality factor was due to a strong magnetolectric coupling in the multiferroic composite core, which led to electric field induced permeability change. The concept of tuning inductance by electric field using multiferroic composite materials leads to a class of compact tunable inductors with minimum power consumption. © 2009 American Institute of Physics.

[DOI: 10.1063/1.3103273]

As one of the three fundamental components for electronic circuits, inductors have been extensively used in a variety of applications, such as power electronics, communication systems, etc. Electrostatically tunable capacitors have been widely used in many different circuit applications. However, electrostatically tunable inductors have not been readily available, which severely limits their applications. A large portion of tunable inductors are magnetically tuned by (electro)magnets, which are bulky, energy consuming, noisy, and inconvenient to use. Efforts have been devoted to developing electronically tunable inductors that have large tunability, high quality factors, and low energy consumption. For example, microelectromechanical systems (MEMS) based tunable inductors<sup>1</sup> can have very high quality factors but they have a limited tunable range of <20% and are difficult to fabricate. Tunable inductors based on magnetic films<sup>2</sup> can have better tunable range but require a constant current that consumes a significant amount of power for tuning, and their quality factors are low.

Multiferroic composite materials having two or more ferroic (ferroelectric, ferro/ferrimagnetic, etc.) phases with strong magnetolectric coupling, i.e., electric field control of magnetic properties as well as magnetic field tuning of electrical polarization<sup>3-5</sup> have great potential for many novel devices such as information storage device,<sup>6</sup> picotesla sensitivity magnetic field sensors,<sup>7,8</sup> and electrostatically tunable signal processing devices, such as resonators,<sup>9</sup> phase shifters,<sup>10</sup> filters,<sup>11</sup> etc. The capability of tuning magnetic properties by electric field (or vice versa) with minimum power consumption makes such multiferroic composites ideal for tunable inductor application. Recently, Fang *et al.*<sup>12</sup> have reported a multiferroic composite consisting of a bar of lead zirconate titanate (PZT) and a ring of MnZn ferrite that showed a change in the inductance of up to 20%. However, its tunability and operational frequencies are still limited.

In this work, electrostatically tunable magnetolectric inductors with multiferroic composite core consisting of two layers of amorphous magnetic ribbons (Metglas 2605CO<sup>TM</sup>) and one PZT (PI Ceramic PIC151) slab have been demonstrated to have a large tunable inductance range of up to

450%. A significant improvement of the quality factor with increasing external electric field has also been observed.

Solenoid type magnetolectric inductors with a layered multiferroic composite core were made, as schematically shown in Fig. 1. The multiferroic composite inductor core consists of two layers of Metglas 2605CO<sup>TM</sup> (~23  $\mu\text{m}$  thick each) magnetic ribbons and one PZT (~0.5 mm thick) piezoelectric slab that was poled along its thickness direction were bonded together with ethyl cyanoacrylate glue. The working coil shown in Fig. 1 was then connected to a precision impedance analyzer (Agilent 4294A) for inductance and quality factor analysis. A control voltage ranging from 0 to 600 V, which results in an electric field from 0 to 12 kV/cm in the PZT slab, was applied across the thickness direction of the PZT slab.

Figure 2 shows the inductance versus frequency curve of the magnetolectric inductor measured under different electric fields. Without the electric field, the inductance of the magnetolectric inductor starts at about 0.2 mH at low frequency (<10 kHz) and rolls off quickly at higher frequencies. Such inductance roll-off behavior is closely related to the large eddy current screening effect associated with the Metglas magnetic ribbons, which reduces the its effective high frequency permeability.<sup>13</sup> A strong electric field dependence of the inductance can be observed, with the inductance decreasing rapidly at higher electric fields. The inductance tunability, which is defined as  $\Delta L/L_{\min}$  at different frequencies is indicated in Fig. 3. Clearly, the inductance values show much larger changes at low frequencies when eddy current effect is not significant. The maximum change of the inductance is about 450%, 250%, and 50% for operation frequencies of 100 Hz, 100 kHz, and 5 MHz, respectively. The energy consumption associated with inductance tuning at maximum electric field of 12 kV/cm can be estimated from the energy associated with charging the PZT capacitor

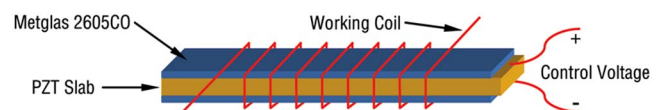


FIG. 1. (Color online) Schematic of the magnetolectric inductor with a multiferroic composite core.

<sup>a)</sup>Electronic mail: nian@ece.neu.edu.

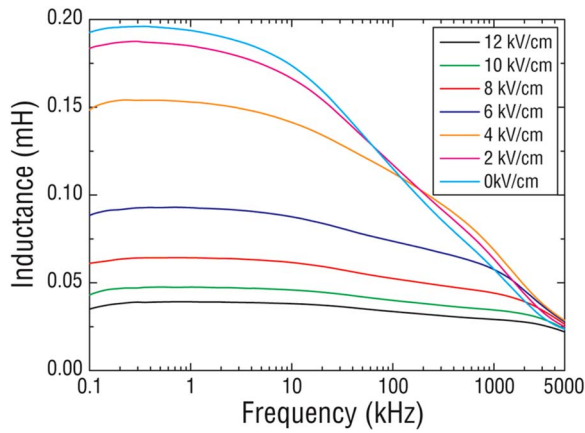


FIG. 2. (Color online) Inductance spectra of the magnetolectric inductor with different electric field applied across the thickness direction of the PZT slab.

with  $E=1/2 \times CV^2$ , where  $C$  is the capacitance of the PZT slab and  $V$  the applied voltage. The estimated energy consumption to achieve maximum tuning is only about 1.3 mJ, which is negligibly small, indicating that these magnetolectric inductors are essentially passive devices. The change of inductance of 450% with negligible power consumption is the largest inductance tunability in passive tunable inductors that ever reported.

The quality factor of the magnetolectric inductor also changes with external electric fields. As shown in Fig. 4, the peak quality factor was improved from  $\sim 3$  at zero electric field to  $\sim 8.5$  with an external electric field of 12 kV/cm. The reason for such improvement of the quality factors is due to the decrease of permeability and hence increased skin depth and reduced core eddy current loss. In addition, the peak quality factor frequency shifts to a higher frequency with higher electric field, which is also due to the reduced permeability and is preferred for real applications.

The change in the inductance and quality factor of the magnetolectric inductor is closely related to the strain mediated magnetolectric coupling within the multiferroic core material, which leads to electric field induced changes of the permeability of the Metglas ribbons. This is evidenced by the electric field induced magnetic hysteresis loop changes through vibration sample magnetometer (VSM) measurements. Figure 5 shows the magnetic hysteresis loops mea-

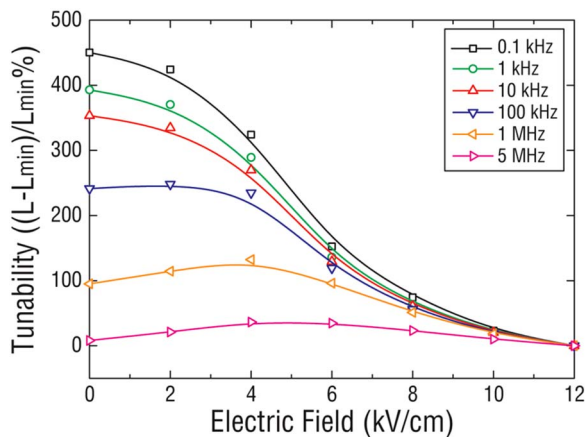


FIG. 3. (Color online) Inductance tunability at different frequencies and electric field.

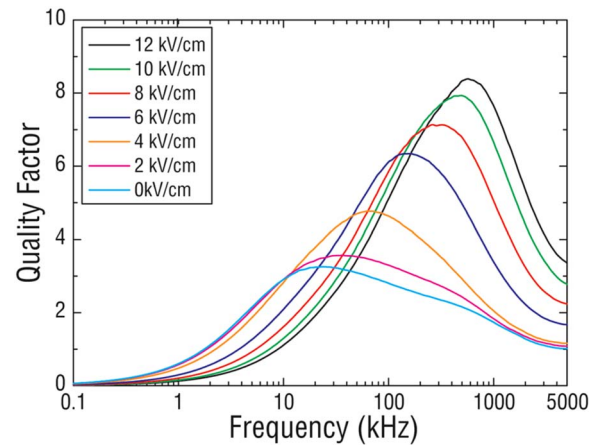


FIG. 4. (Color online) Quality factor spectra of the magnetolectric inductor with different electric field applied across the thickness direction of the PZT slab.

sured along the length direction (also the magnetic flux direction) of the multiferroic composite inductor core with different electric field applied to the PZT slab. Apparently, a low electric field corresponds to a low magnetic anisotropy, while a high electric field results in a high magnetic anisotropy. Since the relative permeability of the magnetic ribbons can be expressed as  $\mu_{\text{eff}}=4\pi M_s/H_{\text{eff}}+1$ , where  $H_{\text{eff}}$  is the total effective anisotropy fields in the magnetic ribbons, a change in the relative permeability, thus a tunable inductance is expected.

The changes in magnetic anisotropy, relative permeability, as well as inductance of the magnetolectric inductor due to the magnetolectric coupling can be estimated by using the inverse magnetoelastic relations. When a positive electric field is applied along the poling direction of the PZT slab, the PZT slab will shrink in the plane of the slab due to its negative piezoelectric coefficient  $d_{31}$ . The deformation will then be transferred to the Metglas magnetic ribbons, leading to induced anisotropy fields. Because of the symmetric long beam structure of the inductor core, while the thickness of the Metglas ribbons are much less than that of the PZT slab ( $t_{\text{mag}}:t_{\text{PZT}} \approx 1:22$ ), the total effective anisotropy fields in the Metglas ribbons due to the inverse magnetoelastic effect can be expressed as (cgs unit),

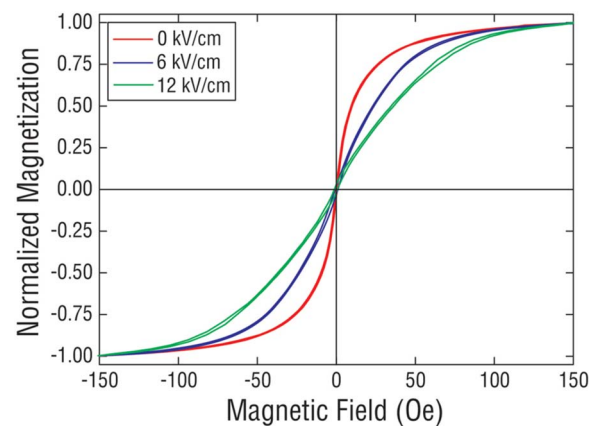


FIG. 5. (Color online) Magnetic hysteresis loops of the multiferroic composite core under different electric fields measured by VSM.

TABLE I. Calculated and measured values of effective magnetic anisotropy and low frequency inductance with difference electric field across the PZT slab (measured at  $\sim 100$  Hz).

E-field (kV/cm)	0	2	4	6	8	10	12
VSM measured $H_{\text{eff}}$ (Oe)	13	24	36	49	60	72	83
Relative permeability	1380	750	500	370	300	250	220
Critical frequency (kHz)	39	72	108	146	180	216	245
Calculated inductance (mH)	0.195	0.111	0.075	0.056	0.048	0.039	0.035
Measured inductance (mH)	0.196	0.187	0.154	0.093	0.064	0.047	0.038

$$H_{\text{eff}} = H_a + H_{ME} = H_a + \frac{3\lambda_s \sigma}{M_s} = H_a + \frac{3\lambda_s Y d_{31} E}{M_s}, \quad (1)$$

where  $H_a$  is the intrinsic in-plane anisotropy field of the Metglas,  $H_{ME}$  is the electric field induced magnetic anisotropy field from magnetoelectric coupling,  $\lambda_s$  is the saturation magnetostriction constant,  $Y$  is the Young's modulus, and  $M_s$  is the saturation magnetization of the magnetic ribbons. Given that the saturation magnetostriction constant of the 2605CO™ Metglas ribbon is  $\sim 35$  ppm, the Young's modulus and saturation magnetization are 100 GPa and 18 kG, respectively,<sup>14</sup> and the piezoelectric coefficient of PZT is  $-200$  pC/N,<sup>15</sup> the theoretical estimated effective magnetic anisotropy field can be made with the above set of parameters, which are comparable to measured values (interpolated from the slope of VSM hysteresis loop) that are listed in Table I. We can see that the electric field induced effective magnetic field is increased with the increment of the electric field, adding to the magnetic anisotropy field of the Metglas ribbons in the multiferroic inductor core. This leads to a reduced permeability and lower inductance at high electric fields, as shown in Figs. 2 and 3.

The inductance of the magnetoelectric inductor at low frequency can be calculated by (assuming a long cylindrical coil),

$$L = \mu_0 \mu_r \frac{N^2 A}{l} = \mu_0 \frac{2\mu_{\text{eff}} t + (d - 2t) N^2 A}{d l}, \quad (2)$$

with  $\mu_r$  being the effective relative permeability of the inductor core,  $N$  is the number of turns of the coil,  $A$  is the cross-section area of the coil,  $l$  is the length of the coil,  $t$  is the total thickness of the Metglas ribbons,  $d$  is the height of the core, and  $\mu_{\text{eff}}$  is the permeability of the magnetic ribbons calculated from  $H_{\text{eff}}$ . The inductance values at low frequencies were calculated from the extrapolated  $H_{\text{eff}}$  values from magnetic hysteresis loops are listed in Table I. The calculated inductance values are close to the measured inductance values from impedance analyzer, except at electric fields of 2 and 4 kV/cm. This discrepancy is likely due to the fact that magnetic domains are much more mobile at low electric field, as shown in the  $B$ - $H$  magnetic hysteresis loops in Fig. 5, leading to large permeability (or inductance) changes at low electric fields. The linearity of the  $B$ - $H$  loops is much better at higher electric fields, which leads to better matching between calculated and measured inductance values. However, at higher frequencies the eddy current loss has to be taken into account, particularly at frequencies when the Metglas layer thickness is larger than its skin depth. Such critical frequency can be easily calculated by  $f = \rho / \pi \mu_0 \mu_r d^2$ , where  $\rho$  is resistivity of Metglas ribbons (123  $\mu\Omega$  cm) and

are listed in Table I as well. These calculated critical frequencies roughly match with the roll-off frequency on the inductance versus frequency curves in Fig. 1.

In conclusion, a magnetoelectric inductor based on multiferroic composite has been made and tested. The inductance tunability, which is mediated by electric field controlled magnetic anisotropy and permeability, achieved a record high value of 450%, 250%, and 50% at 1 kHz, 100 kHz, and 5 MHz, respectively, with minimum power consumptions. The change of the magnetic anisotropy can also be observed in magnetic hysteresis loops. Along with the change of inductance, the quality factor of the tunable inductor also got significantly improved with the increasing of external electric field. It is notable that the performance of such inductors, i.e., operational frequency, quality factor, etc., is severely limited by the excessive eddy current loss due to the relatively large thickness of the magnetic ribbons. The eddy current loss can be reduced by using magnetic/insulator multilayer thin films, which will greatly enhance the performance of such inductors and hence its applicable frequency range. The larger tunability achieved in such multiferroic composite based magnetoelectric inductor with minimum power consumption is ideal for miniaturization and performance optimization of electronic device.

This work is financially supported by NSF under awards 0824008, 0746810, and 0603115 and by ONR under awards N000140710761 and N000140810526.

<sup>1</sup>V. M. Lubecke, B. Barber, E. Chan, D. Lopez, M. I. Gross, and P. Gammel, *IEEE Trans. Microwave Theory Tech.* **49**, 2093 (2001).

<sup>2</sup>M. Vroubel, Z. Yan, B. Rejaei, and J. N. Burghartz, *IEEE Electron Device Lett.* **25**, 787 (2004).

<sup>3</sup>M. Fiebig, *J. Phys. D* **38**, R123 (2005).

<sup>4</sup>W. Eerenstein, N. D. Mathur, and J. F. Scott, *Nature (London)* **442**, 759 (2006).

<sup>5</sup>C. W. Nan, M. I. Bichurin, S. X. Dong, D. Viehland, and G. Srinivasan, *J. Appl. Phys.* **103**, 031101 (2008).

<sup>6</sup>J. F. Scott, *Nature Mater.* **6**, 256 (2007).

<sup>7</sup>S. X. Dong, J. F. Li, and D. Viehland, *Appl. Phys. Lett.* **83**, 2265 (2003).

<sup>8</sup>J. Zhai, Z. Xing, S. X. Dong, J. F. Li, and D. Viehland, *Appl. Phys. Lett.* **88**, 062510 (2006).

<sup>9</sup>Y. K. Fetisov and G. Srinivasana, *Appl. Phys. Lett.* **88**, 143503 (2006).

<sup>10</sup>A. Ustinov, G. Srinivasan, and B. A. Kalinikos, *Appl. Phys. Lett.* **90**, 031913 (2007).

<sup>11</sup>C. Pettiford, S. Dasgupta, J. Lou, S. D. Yoon, and N. X. Sun, *IEEE Trans. Magn.* **43**, 3343 (2007).

<sup>12</sup>X. Fang, N. Zhang, and Z. L. Wang, *Appl. Phys. Lett.* **93**, 102503 (2008).

<sup>13</sup>W. P. Jayasekara, J. A. Bain, and M. H. Kryder, *IEEE Trans. Magn.* **34**, 1438 (1998).

<sup>14</sup>See <http://www.metglas.com> for more information about the properties of Metglas 2605CO™.

<sup>15</sup>See <http://www.physikinstrumente.com/> for more information about the properties of the PIC151 cermaic.